

2101. Study on an engineering measure to improve internal explosion resistance capacity of segmental tunnel lining structures

Yuetang Zhao¹, Cheng Chu², Yijun Yi³

College of Defense Engineering, PLA University of Science and Technology,
Nanjing, Jiangsu Province 210007, P. R. China

State Key Laboratory of Disaster Prevention and Mitigation of Explosion and Impact,
Nanjing, Jiangsu Province 210007, P. R. China

²Corresponding author

E-mail: ¹yuetangzh@163.com, ²iamcci@163.com, ³lgdxyyj@163.com

Received 12 December 2015; received in revised form 22 April 2016; accepted 18 May 2016

DOI <http://dx.doi.org/10.21595/jve.2016.16730>

Abstract. With the increase of terrorist bombing attacks on subway systems, few research results could be traced on the internal explosion capacity of segmental tunnel linings. This paper presented some full-scale test results of segmental tunnel linings under internal explosions, and the deformation and failure patterns of segmental tunnel lining were analyzed and outlined, wherein the key factors and positions that dominate the damage of a segmental lining were figured out. Then based on a conceptual idea, attempts were made, by adding flexible damping cushions on the joints, to relieve the damage degree of contact area of bolts. At last, numerical simulations were performed and it was shown that, the localized failures of joint areas of tunnel segments could be relieved effectively after introduction of this measure, so the internal explosion resistance performance of segmental lining structures could be optimized and hence improved.

Keywords: segmental tunnel lining, internal explosion, full-scale test, joint area, flexible cushion.

1. Introduction

In recently years, as many as thousands of terrorists' bombing attacks took place every year and presents a rising trend around the world. Public transport systems, such as subway transit tunnels, due to the limited space and people crowds, are among the top of the list of targets for terrorists' bombing attacks. The 7 July 2005 London Tube bombing [1], the 2010 Moscow metro bombings [2] and the recent 2016 Brussels metro bombings [3], etc. are the most notorious events. In these attacks, not only huge casualties were caused, but also the structural elements were damaged or destroyed. For a tunnel crossing a river, water may inrush if the tunnel lining were breached by explosion, thus causing far more severe consequences [4]. Since 2004, the International Symposium on Tunnel Safety and Security are held every three years [4], considerable big portions of conference papers were published specially discussing the evaluation and analysis methods, prevention measures and emergency evacuation for Tunnel explosion and fire. In 2006, the American Federal Highway Administration determined a six years bridge and tunnel safety research plan [5], which aimed at building a complete set of consulting and training system of engineering technologies for the resistance to terrorist attacks on bridge and tunnel structures.

Till now, researches about tunnel structures' resistance to terrorist explosion are still relatively scarce and parts of the achievements were not made public due to the military implication. And as for the designing of the structures, except for the defense structures which have special functions, explosive loading is not taken into account when designing civil buildings, while seismic loadings are commonly taken account for those structures in earthquake areas. However, due to the difference in frequencies and intensities between explosive shock loadings and seismic loadings, the response of buildings under these two scenes will quite be also different.

Thanks to the superiority of construction efficiency and small influence on the surface ground, shield tunneling method has been widely used in urban tunnel engineering for areas of soft soil. The most apparent difference between segmental shield tunnel lining and an integral liner lies in

the existence of joints bonding several different types of segments in a ring and rings in the longitudinal direction of a tunnel, which are connected by pre-stressed jointing bolts. Due to the effects of joints, the overall rigidity and loading capacity of segmental lining are relatively low, compared with that of an integral one, also the deformation and damage mechanisms are different. Neither the Japan Society of Civil Engineering nor the International Tunneling Association [6] takes explosive loadings into account in their shield tunnel designing guidelines now. In spite of the small occurrence probability, the risk of terrorists' attacks on tunnel still exist with the development of suicide bombing technology and the possible existence of security system loopholes. Once the bombing occurs, the consequence could be very serious. Localized damage on structural elements could be induced, even the entire tunnel structure may further collapse. As aforementioned, if the tunnel is under a river, water inrush through the breaches and openings of the joints between lining segments may occur and lead to disastrous consequences. Therefore, it is of significance to probe into the behaviors of segmental tunnel lining, and on whose base, to put forward corresponding engineering and technical explosion resistance measures to mitigate the effects from blast loadings.

Y. S. Karinski et al. [7] analyzed the response of circular cross section multi-segmented lining to dynamic loading, considering that for prefabricated linings the stiffness of the joints interconnecting the different segments is usually far smaller than the segments, they proposed a simplified model that the lining is composed of a number of rigid arch segments interconnected by elastic-plastic hinges, and the lining is surrounded by a medium of visco-elastic properties. Liu Mu-yu [8, 9] et al. figured out the weakest part of Wuhan Yangtze river tunnel lining in response to explosion using numerical simulation method, but the calculation ignores bolts and earth pressure. Wu Yu-bin [10] et al. studied the dynamic response characteristic of segment tunnel under internal explosion, a three dimensional FEM model of a typical metro shield tunnel was proposed, in which the contacts between segment to segment, segment to jointing bolts, and lining to soil could be appropriately modeled, the failure characteristics of segments and joints were revealed, and the authors suggested that blast-resistance capacity of shield tunnel could be improved by enhancing jointing bolts strength and tenacity. In a word, direct research results for reference are scarce, and no published full-scale or model tests could be traced, thus those results from numerical methods are not validated against.

In this paper, to begin with, full-scale test results of internal explosion on vertically staggered assembled segmental linings were briefly introduced. Then, the failure patterns of segmental lining were revealed, which provides the basis for the proposal of measures to improve blast-resistance capacity of the structure in the next step. At last, the measure was put forward and its effectiveness was verified through numerical calculations. Analyses were made and concluding remarks could be made as follows: the deformation localization on joint areas could be relieved dramatically by introduction of damping cushions, thus considerably optimizing the internal explosion resistance performance of segmental lining structures.

2. Full-scale test results of vertically assembled shield tunnel lining

There exist many researches related to the deformation patterns of shield segmental lining structure. JanBen [11] thinks segment movement could be treated as rigid body motion since the joint stiffness is far smaller, and the behavior of a segment joint, together with the jointing bolt, could be modeled by a torsional spring hinge, which presents a nonlinear dependence between the bending moment on it and the relative rotation angle. Ngoc Anh DO et al. [12-16], on the basis of structure matrix method, took the effects of segmental joints into account, systematically studied the dynamic response of segmental lining structures. However, since the loads were seismic wave loads whose frequency is relatively low, the structure response was obtained through pseudo-static method. Matteo Colombo et al. [17, 18] think that lining segment has an outward motion trend under the effect of internal blast loading, so they adopted tensile springs to model the segmental joints, and gave a group of P-I curves for segment lining under internal explosion after a number

of numerical calculations by ABAQUS software. However, none of these outcomes are validated against any test results.

Due to the difficulty and risks of tests, no published results can be traced on segmental tunnel's response to internal explosions. To study the true dynamic response of shield segmental lining structure, and provide data and results for validation for further simplified mathematical models and numerical simulations, the authors conducted a series of tests on full-scale models.

2.1. Outlines of the test

We take the widely acceptable vertical assemblage [19] for shield fabricated linings. Two parallel tunnels were vertically assembled at a testing field (see Fig. 1(a)), each is composed of four staggered rings, and each ring consists of 3 A type segments, 2 B type segments and 1 K segment (see Fig. 1(b)). The ring has a diameter of 6.3 m at extrados and 5.5 m at intrados with a radial thickness of 0.4 m, and its height in tunnel axial direction is 1.2 m. All of the segments are prefabricated by Nanjing Dadi Construction Factory for Nanjing subway engineering.

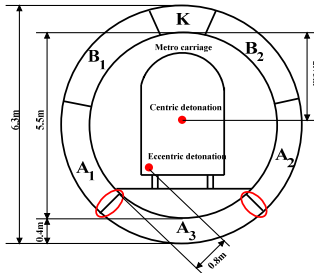
Given a certain structure, its response to explosion is determined by the type, size, location and ignition method of the charge, as for our problem, these however are determined by the terrorists. According to Federal Emergency Management Agency-Fema2005 [20], for the purpose of protective design, the capacity of a briefcase, a suitcase can be referenced in Table 1. In our tests, the maximum charge weight is set as 20 kg, whereas multiple sources are beyond our scope of study.

Table 1. Capacity of explosion resistance

Threat Description	Explosive Mass (TNT Equivalent)
Pipe Bomb	2.3 kg
Suicide Belt	4.5 kg
Suicide Vest	9 kg
Briefcase/Suitcase Bomb	23 kg



a) Layout at fields



b) Schematic diagram of internal blast test



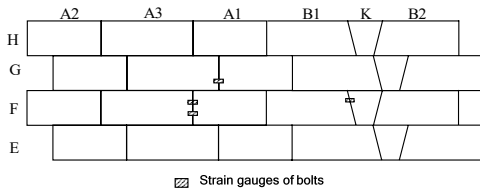
c) Position of explosive charge

Fig. 1. Full-scale model test set-up

Central ignition method was adopted and the distance from the charge center to the closest lining interior surface is 0.8 m, as illustrated in Fig. 1. The eccentric location of explosive is determined by the principle of the most adverse condition according to the geometric characteristic of a typical Nanjing metro carriage. The corner of the carriage is closest to lining interior surface, namely the joint contact area of A3 segment and A1 segment (or A2 segment). It is reasonable to understand that lining would behave differently to centric detonation and eccentric one. Some

researchers only consider a centric detonation scenario; in that way the loading is underestimated for the near-field structural elements.

In this paper, the authors mainly focused on the strain of bolts closest and farthest to the explosive. Fig. 2 shows the arrangement of strain gauges.



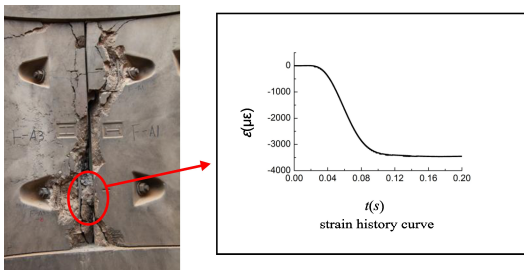
a) Schematic diagram of layout

b) Strain gauge on bolt

Fig. 2. Arrangement of strain gauges

2.2. Test results analysis

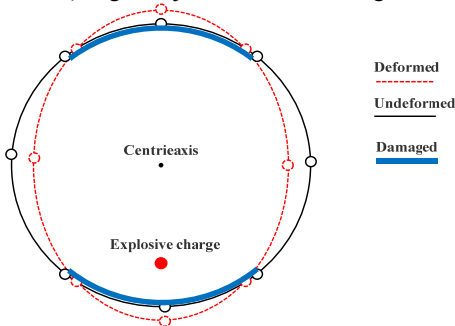
By observing the test results, the basic failure patterns can be outlined. For both centric and eccentric detonations, only localized damages occurred in the joint areas. Especially for the eccentric detonation test, the joint of A3-A1 and the joints along the successive boundaries of the key segments were damaged seriously and presented a crushing destruction, as shown in Fig. 3(a) and Fig. 3(b). Moreover, the bolts deformed so largely that they tended to be straightened and the washers were partly embedded in the concrete. As demonstrated in Fig. 3(d), the damages of other areas focused on the segment joints, mainly presented the crash of concrete outside reinforcement. There were no obvious deformation and damage phenomena in main part of segments and adjacent rings. Fig. 3(c) shows the overall elliptical deformation pattern of the lining ring under the eccentric detonation, this is due to larger loads on near-field and far-field areas. The larger change of curve ratio for near-field area contributes to the damage of the zones (see Fig. 3(b)).



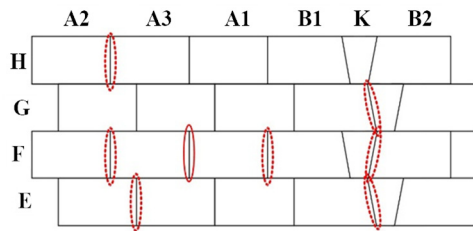
a) Segment joint of A3-A1 in ring F



b) Segment joint of K-B2 in ring F



c) Elliptical deformation under eccentric detonation



d) Damage in joint areas

Fig. 3. Damage of segments

The unrecoverable deformation of strain gauges on the circumferential bolts of A1-A3 joint of

F ring is shown in Fig. 3(a). The curve in Fig. 3(a) represents the strain history of strain gauge in the middle of circumferential bolt closest to the explosive source, from which we can find that the unrecoverable deformation is $3431 \mu\epsilon$.

From the test results, characteristics of segmental lining's dynamic response can be outlined as follows:

1. For both centric and eccentric detonations, the damages localized in the contact areas of joints, meanwhile the ring where explosive charge locates damaged most severely.
2. Stress concentration is produced in the contact area of joints due to the binding effect of circumferential bolts on the outward movement of segment under internal explosive loadings. And stress concentration contributes to failure of concrete and bolts in joint areas.
3. The lining mainly expand outward under the effect of internal explosion, while the deformation in the axial direction is much smaller, which can be supported by the test results that damage on ring joints are minute.
4. Under eccentric detonation, the overall deformation of lining ring is an elliptical pattern with the line connecting, the near-field and far-field as the long axis of the ellipse. So the curve ratio of the intrados of lining increases for the near-field and far-field, which intensify the damage on these areas.

3. Measure to improve internal explosion resistance capacity of segmental lining structures

3.1. Basic conceptual ideas

As aforementioned, under internal explosive loading, local binding forces of the bolts are the main reason for stress concentration on joint areas. If the stress concentration can be reduced, then damage in the joint areas should be mitigated, thus improving internal blast-resistance of segmental tunnel linings.

The idea to increase explosion resistance can be preliminarily summarized as follow. On the premise of meeting the requirement of security and stability in daily operation, stress concentration of the contact area of joints under internal explosion could be reduced by certain measures. Under the effect of internal explosive loadings, because of the outward motion of lining segments, the fastening forces on bolts rise. We want it rise below a threshold so that the reinforced concrete in the joint areas will not be damaged, this demands more allowable displacement for the segments bonded together by the jointing bolts. Under the requirements of safe operation and low costs, an effective measure is adopting flexible fastening technology.

The flexible fastening technology of bolts has the characteristics of large deformation, strong energy absorption effects and good deformation compensation ability under stress, so it can withstand the shock loads, vibration loads or thermal loads. The authors propose adding flexible cushion (as shown in Fig. 4) or washer (as shown in Fig. 5) to the joints, thus large deformation is allowed under the dynamic loads and in turn prolong the working time of the impulse, thus damping the amplitude of the loads. The Japan Society of Civil Engineering recommends to apply carbamic acid polyester washer in the jointing bolts to improving seismic resistance performance of segmental lining structures [21], where the mechanism is similar.

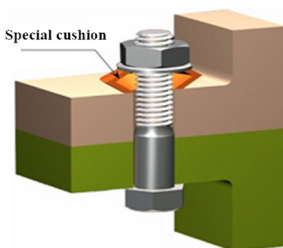
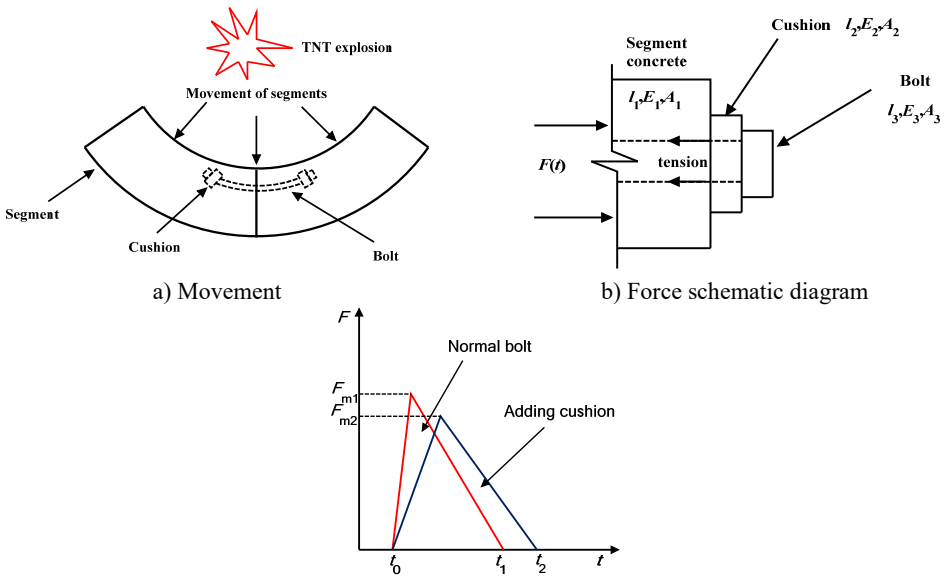


Fig. 4. Elastic cushion



Fig. 5. Carbamic acid polyester flexible cushion



c) Force histories of a normal bolt and one with cushion
Fig. 6. Schematic diagram of joint area closest to explosive

Fig. 6 represents the schematic diagram of joint area closest to the explosive. Under internal explosive loading $F(t)$, the segments will move outwards (see Fig. 6(a)), thus causing the adjoining bolts be stretched, while concrete and cushion compressed (see Fig. 6(b)). With the same impulse that works on the bolt, and with the compressible cushion added, the working time is prolonged, this in turn decreases the magnitude of reaction force on the bolt. The bolt extension can be conceptually expressed as follows:

$$\Delta l = \int_{t_0}^{t_e} \frac{F(t)l_3}{E_3A_3} dt = \frac{l_3}{E_3A_3} \int_{t_0}^{t_e} F(t) dt = \frac{I_m l_3}{E_3A_3}, \tag{1}$$

where t_0 and t_e represent the arriving and ending time of shock wave, respectively; EA represents the stiffness, l represents length; I_m is the assumed impulse of the explosive loading that works on this bolt. Once I_m is fixed, Δl is determined. If we assume that there is no opening (which we desire for the waterproof of the tunnel) between segments, bolt-cushion-segment, then we will also have:

$$\Delta l = \int_{t_0}^{t_e} \left(\frac{F(t)l_1}{E_1A_1} + \frac{F(t)l_2}{E_2A_2} \right) dt = \frac{l_1}{E_1A_1} \int_{t_0}^{t_e} F(t) dt + \frac{l_2}{E_2A_2} \int_{t_0}^{t_e} F(t) dt = \left(\frac{l_1}{E_1A_1} + \frac{l_2}{E_2A_2} \right) I_m. \tag{2}$$

Since $E_1 \gg E_2$ (as shown in section 3.2.2), a large proportion of Δl will be distributed on the more flexible cushion, which means, the strain of the concrete is drastically relieved.

In other words, after the introduction of flexible cushion, the deformation will be mainly concentrated on the cushion. Thus explosive energy will be more absorbed by the elastic cushion, the stress concentration on segment corners will be relieved, so the resistance performance improved.

3.2. Verification by numerical calculations

In this subsection, the effectiveness of the proposal is verified by numerical simulations, which were performed by nonlinear dynamic FE code of LS-DYNA.

3.2.1. FE model

The tests showed that the damages mainly appear in the ring where the explosive locates. To simplify the calculation, only one ring of segment was taken into account and the effect of longitudinal bolts was ignored. The simplification would increase the internal force and deformation of segments to some extent, so the analysis is conservative.

The simulation took the method of Arbitrary Lagrange Euler to consider the coupling effect between the explosion products, air and the structure. The finite element model is shown in Fig. 7, where the mesh of air is not presented for showing, the air and explosive constituted Euler area, meanwhile the segments, soil, bolts and cushions constituted Lagrange area, air mesh covers the segmental lining. Automatic single face contact method was adopted to model the effect on the interfaces between soil and lining, segments and segments, segments and bolts, etc. The exterior of the soil part is set to be a transmitting boundary to simulate infinite media.

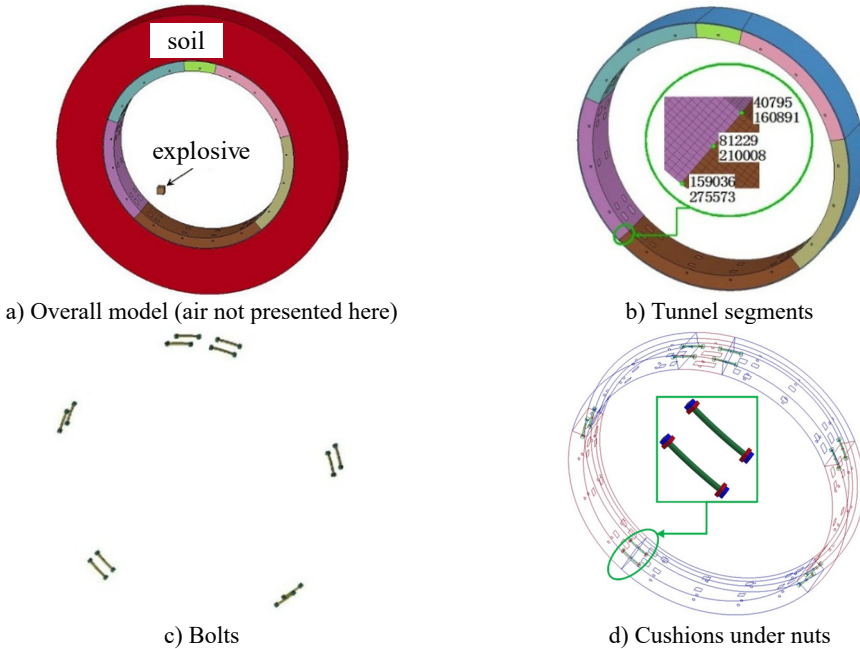


Fig. 7. FE model

3.2.2. Materials model

Before applying explosive loadings, the preload of jointing bolts' fastening force should be applied. In this paper, 3000 N of fastening forces were applied on the bolts by iterative calculation method. The bolts were modeled by the PLASTIC_KINEMATIC model and soil by MORH-COLOMB model. The concrete segments were modeled by PESUDO_TENSOR model [22] (as shown in Fig. 8). The PESUDO_TENSOR model includes two curves respectively, the upper one is the maximum yield curve and the lower one is the failed material curve. σ_{\max} and σ_{failed} are expressed as Eq. (3) and Eq. (4), where p is pressure, respectively. a_0 , a_1 , a_2 , a_{0f} and a_{1f} are material parameters respectively.

$$\sigma_{\max} = a_0 + \frac{p}{a_1 + a_2 p}, \quad (3)$$

$$\sigma_{\text{failed}} = a_{0f} + \frac{p}{a_{1f} + a_2 p}. \quad (4)$$

The material parameters [23] were listed in Table 2, Table 3 and Table 4, where RO, E, PR (or RUN), SIGY, ETAN, BETA, G, GMOD, PHI and CVAL (or A0) represent mass density, Yong modulus, Poisson’s ratio, yield stress, tangent modulus, hardening coefficient, shear modulus, elastic shear modulus, angle of friction and cohesion value, respectively. A1 and A2 are hardening coefficients, A0F and A1F are failure hardening coefficients.

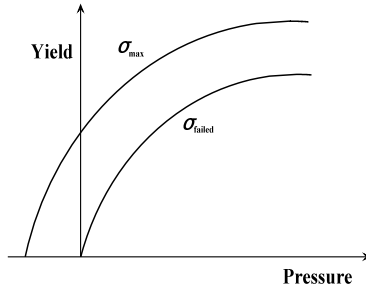


Fig. 8. Two-curve model with damage and failure

The equation of state of JWL, which is expressed as Eq. (5) [22] was used to described the detonation products of TNT.

$$p = A \exp(-R_1 V) + B \exp(-R_2 V) + \frac{\omega}{V} \left[E - \frac{A}{R_1} \exp(-R_1 V) - \frac{B}{R_2} \exp(-R_2 V) \right], \quad (5)$$

where $V = \frac{\rho_0}{\rho}$ is relative volume, $E = \rho_0 e$ is detonation energy per unit volume. A, B, R_1, R_2 and ω are coefficients of equation and they are constants in a given explosion simulation.

The parameters of Equation of state for TNT explosive are illustrated in Table 5.

Table 2. Materials’ parameters of bolts

Material	RO (kg/m ³)	E (Pa)	PR	SIGY (Pa)	ETAN (Pa)	BETA
Bolt (M30)	7800	2.1e11	0.238	3e8	2.1e9	0.5

Table 3. Materials’ parameters of soil

Material	RO (kg/ m ³)	GMOD (Pa)	RUN	PHI	CVAL (Pa)	E
Unsaturated soil	1650	7.4e6	0.3	0.45	e5	3.0e7

Table 4. Materials’ parameters of tunnel segments

Material	RO (kg/m ³)	G (Pa)	PR	SIGF (Pa)	A0 (Pa)	A1	A2	A0F (Pa)	A1F
Concrete (C50)	2650	2.13e10	0.2	6.44e7	1.35e7	1	0	0	0.385

Table 5. Parameters of Equation of state for TNT explosive

Explosive type	A (GPa)	B (GPa)	C (GPa)	R ₁	R ₂	ω
TNT	371.2	3.231	1.054	4.15	0.95	0.30

The air was described by the equation of state for ideal gas which is express as Eq. (6) [22]:

$$p = (\gamma + 1)\rho e, \quad (6)$$

where p is gas pressure (unit: Pa), γ is the ratio of specific heats whose value was 1.4 in this paper, ρ is mass density with value of 1.225 kg/m³, e is internal energy per unit volume, here values 4192 MJ/m³.

The main function of cushion (or washer) is to adjust fastening force of joint during the motion process. In this paper, three working conditions were considered during the numerical calculation, as listed in Table 6. As shown in Fig. 7(d), the cushions were placed on the contact area of joints

closest to the explosive. The cushions made of carbamic acid polyester were simulated by SOIL_AND_FOAM model. A typical mechanical characteristic curves of cushion were shown in Fig. 9. The material parameters of carbamic acid polyester cushion from the reference [24-26] listed in Table 7 (after conversion) were used in calculations, where RO and G represent mass density and shear modulus, respectively. A0, A1 and A2 are the coefficients of yield function.

Table 6. List of working conditions

Number	Working conditions
1	Normal fastening bolts, initial fastening forces were set as 3000 N
2	Adding cushion (thickness 3.8 cm), initial fastening forces were set as 3000 N
3	Removing bolts closest to explosive, namely fastening forces identically equal to 0

Table 7. Parameters of cushion model

Material	RO (kg/m ³)	G (Pa)	A0 (Pa ²)	A1 (Pa)	A2
Carbamic acid polyester	1150	13.8e6	1.21e15	2.018e7	0.084

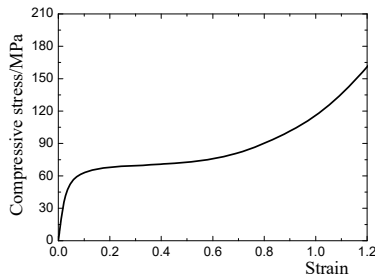


Fig. 9. Typical mechanical properties of cushion [26]

4. Results and discussions

4.1. FEM results analysis

Fig. 10 shows the plastic strain fringe plot in different working conditions and the stripe levels are the same. All the joint areas appear obvious plastic deformation and maxima plastic strains locate in joint areas (shown in Table 8). It can be observed that plastic areas and plastic strain maxima with ordinary bolts are obviously bigger than that of other working conditions. After adding cushions, plastic areas and plastic strain peak values of joint areas decreased. Meanwhile, the plastic strain of bolts far away from the explosive was not obvious. When the two circumferential bolts closest to the explosive source were removed, the plastic area and plastic strain peak values were almost the same with that of adding cushions. The analyses above suggest that appropriate relaxation of fastening condition can greatly reduce the damage of segments.

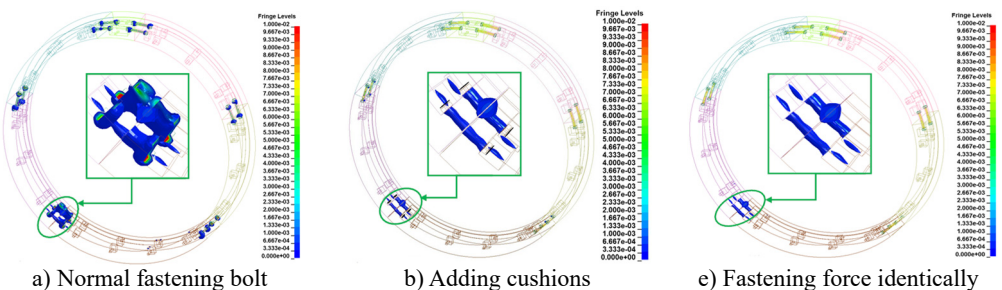


Fig. 10. Plastic strain contours of tunnel segments in different fastening conditions

Table 8. List of maximum effective plastic strain

Working condition number	ϵ_{pm} ($\mu\epsilon$)
1	104518
2	4861
3	4317

Fig. 11 represents the movement of segments, where the node groups were shown in Fig. 7(b). The history curves of distances between two corresponding nodes were shown in Fig. 11, from which we can find that the opening displacement when adopting ordinary bolts is obvious smaller than other conditions. The former displacement is 3 times of the latter and the trend of history curves is different from each other. In addition, adding cushions or removing the bolts closest to the explosive, relative displacement of joints changed little, what is in accordance with the evolution rules of plastic strain analyzed.

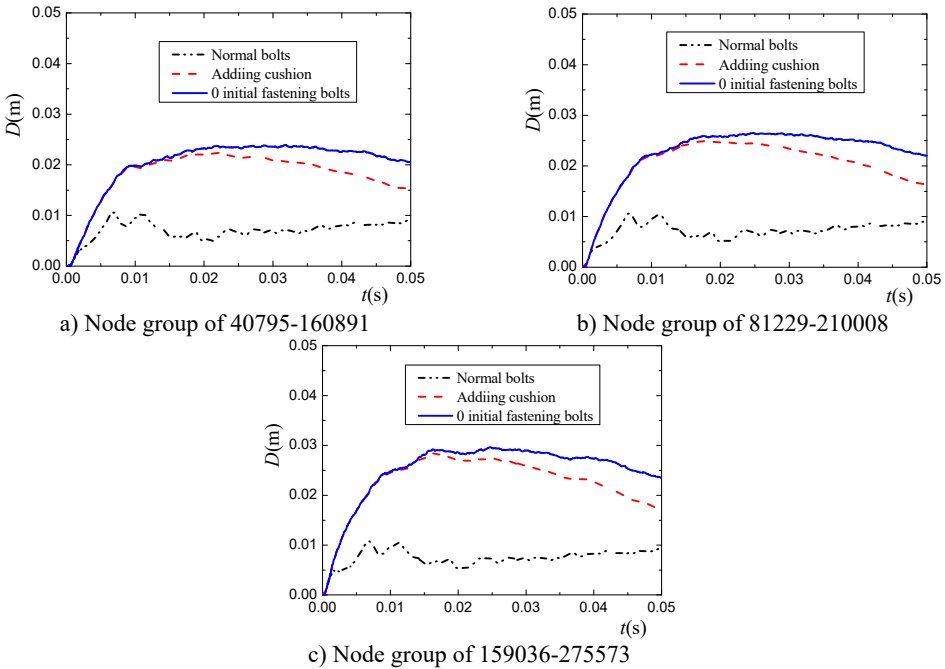


Fig. 11. Opening displacement of tunnel segments in different working conditions

As shown in Fig. 3(a), the maximum axis strain of circumferential bolts closest to explosion source is 3431 $\mu\epsilon$. The diameter of bolt is 3 cm, so the fastening force corresponding to the strain can be calculated as 490000 N. Fig. 12 represents the fastening force history of bolt, from it, we can find that the maximum fastening force is about 900000 N when adopting normal bolts, which is different from the test data. Analysis shows that the difference is mainly caused by the constraint of surrounding segments in the test. The constraint will decrease the outward movement and deformation of the segments closest to the explosive, thus the destruction of explosion will be decreased in some extent. Moreover, because of the existence of constraint fraction, the fastening force tested from the experiment remained unchanged after the maximum value, as shown in Fig. 3(a). However, the fastening force calculated from the numerical simulation will restore in some extent for not taking the constraint into account. When adding cushions, the maximum value of fastening force is about 200000 N, which is less than the force of normal bolts, and in practical engineering, the value will must be less for the existence of constraints from surrounding segments.

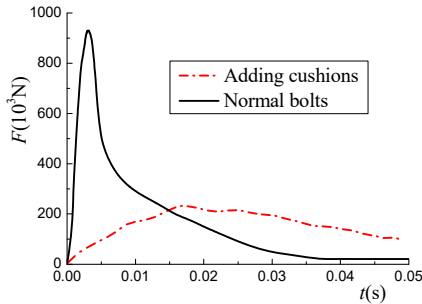


Fig. 12. Fastening force history of bolt

4.2. Engineering application of cushion

Analyses show that the adoption of flexible cushion can reduce the restraint stiffness of joint area of segments, so the destruction of joint area can be greatly decreased under explosion load. In engineering, the design of cushion or washer should meet the following demands:

- 1) Satisfy the requirement of necessary fastening force in daily operation;
- 2) The stress relaxation should be small;
- 3) The system of bolts and cushions can provide the necessary displacement under the explosion load and irreparable damage to the segment structure should not be caused by the enhanced fastening force.

Fig. 13 represents the typical compression curve of cushion, where S_0 and F_0 represent fastening displacement and fastening force, respectively. S_m and F_m represent maximum compression displacement and corresponding fastening force the cushion can provide, respectively. Calculation shows that the maximum opening displacement of joint is about 3 cm when the fastening force of single circumferential bolt is less than 200000 N, so if the displacement of a single cushion can provide is more than 1.5 cm then the plastic strain of segments will be limited in a small range, and the fastening force during compression progress is less than 200000 N.

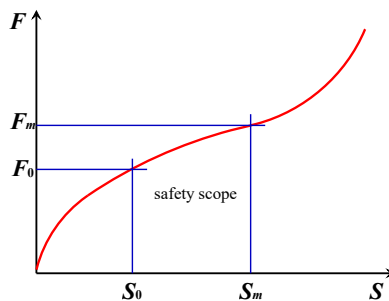


Fig. 13. Mechanical properties of washer or cushion

The segmental lining structure studied above was assembled vertically, while in practice projects the structure is assembled horizontally. Luo [27] studied the difference, and showed that the degree of damage for the structure assembled horizontally is relative smaller for the effect of soil constraint when the charge condition is the same, so the authors' test results are more conservative.

5. Conclusions

In this paper, full-scale model tests of segmental lining structure under the effect of internal explosion were presented, from which the deformation and damage modes of multi-segment lining

were outlined. The key positions that control the failure of the structure were figured out and an engineering measure which can relieve the destructive effect of explosion was proposed, and then the proposal was preliminarily verified by numerical calculations. The main conclusions are as follows:

1. Full-scale model tests showed that the destruction of segmental lining structure was mainly focused in the joint areas closest to the explosive. The stiffness of segment is far larger than the joint area, thus obvious deformation and stress concentration in the across area of circumferential bolts, which lead to local destruction when the failure criterion of concrete is reached.

2. On the basis of the analysis of deformation and failure modes for segment lining structure, the method of decreasing restraint stiffness of circumferential bolts closest to the explosive was proposed to reduce the effect of explosion destruction. Reducing the constraint stiffness of circumferential bolts, the cushion will be compressed and relative movement between segments will take place. During this process, the acting time is prolonged. Given the same amount of impulse from the explosion, the amplitude of the acting force is damped, so the internal force of segments and bolts will decrease. Numerical analyses show that, by this way, not only the plastic strain peak values, but also the areas of plasticity can be effectively reduced. The conclusion implies significance for the fast repair of the structures and the restoration of the traffic after explosion attacks.

3. The adoption of flexible cushions or washers with special function to the joint bolting system can effectively reduce the constraint stiffness of circumferential bolts, with the merits of low costs and easy installation. The proposed measure should be further verified by simplified analyses and tests. Moreover, the production progress and the maneuverability should also be optimized before applications.

Acknowledgements

The study is supported by the National Science Foundation of China (No. 51478469 and No. 51021001).

References

- [1] 7 July 2005 London Bombings. Wikipedia, 2005.
- [2] 2010 Moscow Metro Bombings. Wikipedia, 2010.
- [3] 2016 Brussels Bombings. Wikipedia, 2016.
- [4] **Zhao Y. T., Lin J. W., Shi L.** Research status of terrorist explosion in subway. The Proceedings of the Second National Conference on Engineering Safety and Protection, Vol. 1, 2010, p. 210-213.
- [5] **Parsons, Brinckerhoff, Quade, et al.** Making Transportation Tunnels Safe and Secure. Transportation Research Board, Report 525, Vol. 12, 2006, p. 232-245.
- [6] **No W. G.** Guidelines for the design of shield tunnel lining. Tunnelling and Underground Space Technology, Vol. 15, 2000, p. 303-331.
- [7] **Karinski Y. S., Yankelevsky D. Z.** Dynamic analysis of an elastic-plastic multisegment lining buried in soil. Engineering Structures, Vol. 29, 2007, p. 317-328.
- [8] **Lu Z. F., Liu M. Y.** Analysis of dynamic response and structure damage of Yangtze River tunnel subjected to different explosion loading. Blasting, Vol. 30, 2013, p. 5-9.
- [9] **Liu M. Y., Lu Z. F.** Analysis of dynamic response of Yangtze River tunnel subjected to contact explosion loading. Journal of Wuhan University of Technology, Vol. 29, 2007, p. 113-117.
- [10] **Wu Y. B., Liu R. S., Tian Z. M.** Analysis on dynamic response of a shield tunnel under internal explosion loading. Journal of Wuhan University of Technology, Vol. 33, 2011, p. 107-111.
- [11] **Janben P.** Load Capacity of Segment Joints. Ph.D. Thesis, Braunschweig University of Technology, 1983.
- [12] **Do N. A.** Numerical Analyses of Segmental Tunnel Lining under Static and Dynamic Loads. Ph.D. Thesis, INSA, 2014.
- [13] **Do N. A., Dias D., Oreste P., et al.** Three-dimensional numerical simulation of a mechanized twin tunnels in soft ground. Tunnelling and Underground Space Technology, Vol. 42, 2014, p. 40-51.

- [14] **Do N. A., Dias D., Oreste P., et al.** 2D numerical investigation of segmental tunnel lining under seismic loading. *Soil Dynamics and Earthquake Engineering*, Vol. 72, 2015, p. 66-76.
- [15] **Do N. A., Dias D., Oreste P., et al.** A new numerical approach to the hyperstatic reaction method for segmental tunnel linings. *International Journal for Numerical and Analytical Methods in Geomechanics*, Vol. 38, 2014, p. 1617-1632.
- [16] **Do N. A., Dias D., Oreste P., et al.** 2D numerical investigation of segmental tunnel lining behavior. *Tunnelling and Underground Space Technology*, Vol. 37, 2013, p. 115-127.
- [17] **Colombo M., Martinelli P., di Prisco M.** A design approach for tunnels exposed to blast and fire. *Structural Concrete*, Vol. 16, Issue 2, 2015, p. 262-272.
- [18] **Colombo M., Martinelli P., Huaping R.** Pressure-impulse diagrams for SFRC underground tunnels. *Computational Modelling of Concrete Structures – Proceedings of EURO-C*, Vol. 2, 2014.
- [19] **Blom C. B. M.** *Design Philosophy of Concrete Linings for Tunnels in Soft Soils*. TU Delft, Delft University of Technology, 2002.
- [20] *Design Guidance for Shelters and Safe Rooms-Providing Protection to People and Buildings Against Terrorist Attacks*. Fema, 2005.
- [21] **Koizumi A.** *The Study on Earthquake-Resistant Behavior of Shield Tunnel and Examples*. China Architecture and Building Press, 2009, p. 248-249.
- [22] **Halquist J. O.** *LS-DYNA Keyword User's Manual Version 971*. Livermore Software Technology Corporation, Livermore, CA, 2007.
- [23] **Luo K. S., Zhao Y. T., Luo Z. X.** Numerical simulation on initial stress and strain state of subway segmented tunnel. *China Civil Engineering Journal*, Vol. 46, 2013, p. 78-84.
- [24] **Kong X. P., Jiang Z., Yang L., et al.** A numerical study on adhesive layer effects and the protection capability of ceramic composite armors against multi-hit. *Engineering Mechanics*, Vol. 2, 2012.
- [25] **Prisacariu C., Buckley C. P., Caraculacu A. A.** Mechanical response of dibenzyl-based polyurethanes with diol chain extension. *Polymer*, Vol. 46, 2005, p. 3884-3894.
- [26] **Yi J., Boyce M. C., Lee G. F., et al.** Large deformation rate-dependent stress-strain behavior of polyurea and polyurethanes. *Polymer*, Vol. 47, 2006, p. 319-329.
- [27] **Luo Z. X.** *Theoretical and experimental research on cross-river segmental lining under internal explosion*. PLA University of Science and Technology, 2012, p. 19-35.



Yuetang Zhao received Ph.D. degree from PLA University of Science and Technology, Nanjing, China, in 1996. Now he works at State Key Laboratory of Disaster Prevention and Mitigation of Explosion and Impact. His current research interests include explosion and impact dynamics, underground protective structures.



Cheng Chu received Bachelor's degree of Civil Engineering in Hunan University, Changsha, China in 2010 and Master's degree of Structural Engineering in PLA University of Science and Technology, Nanjing, China in 2013. Now he's working on Ph.D. degree at PLA University of Science and Technology. His current research interests include explosion and impact dynamics, underground protective structures.



Yijun Yi received Bachelor's degree of Civil Engineering in Tianjin University, Tianjin, China in 2013. Now he's working on Master's degree at PLA University of Science and Technology. His current research interests include explosion and impact dynamics, underground protective structures.